Functional diversification of centrins and cell morphological complexity

Delphine Gogendeau[1,2,3,*], Catherine Klotz[1,2,3], Olivier Arnaiz[1,2,3], Agata Malinowska[4], Michal Dadlez[4,5], Nicole Garreau de Loubresse[1,2,3], Françoise Ruiz[1,2,3], France Koll[1,2,3] and Janine Beisson[1,2,3]

[1]CNRS, Centre de Génétique Moléculaire, UPR 2167, Gif-sur-Yvette, F-91198, France
[2]Université Paris-Sud, Orsay, Paris, F-91405, France
[3]Université Pierre et Marie Curie, Paris 6, F-75005, France
[4]Mass Spectrometry Laboratory, Institute of Biochemistry and Biophysics, Polish Academy of Sciences, 02-106 Warsaw Pawinskiego 5a, Poland
[5]Department of Biology, University of Warsaw, ul. Miecznikowa 3, 02-091 Warsaw, Poland
*Author for correspondence (e-mail: gogendeau@cgm.cnrs-gif.fr)

Accepted 9 October 2007
Journal of Cell Science 121, 65-74 Published by The Company of Biologists 2008
doi:10.1242/jcs.019414

Summary

In addition to their key role in the duplication of microtubule organising centres (MTOCs), centrins are major constituents of diverse MTOC-associated contractile arrays. A centrin partner, Sfi1p, has been characterised in yeast as a large protein carrying multiple centrin-binding sites, suggesting a model for centrin-mediated Ca^{2+}-induced contractility and for the duplication of MTOCs. In vivo validation of this model has been obtained in *Paramecium*, which possesses an extended contractile array – the infraciliary lattice (ICL) – essentially composed of centrins and a huge Sfi1p-like protein, PtCenBP1p, which is essential for ICL assembly and contractility. The high molecular diversity revealed here by the proteomic analysis of the ICL, including ten subfamilies of centrins and two subfamilies of Sf1p-like proteins, led us to address the question of the functional redundancy, either between the centrin-binding proteins or between the centrin subfamilies. We show that all are essential for ICL biogenesis. The two centrin-binding protein subfamilies and nine of the centrin subfamilies are ICL specific and play a role in its molecular and supramolecular architecture. The tenth and most conserved centrin subfamily is present at three cortical locations (ICL, basal bodies and contractile vacuole pores) and might play a role in coordinating duplication and positioning of cortical organelles.

Supplementary material available online at
http://jcs.biologists.org/cgi/content/full/121/1/65/DC1

Key words: Basal bodies, Centrin, Centrin-binding proteins, Cytoskeleton organisation, *Paramecium*

Introduction

Centrins are Ca^{2+}-binding proteins that are ubiquitous in eukaryotic cells. They have long been shown to localise at two major sites: microtubule organising centres (MTOCs), for example, spindle pole bodies, centrosomes or basal bodies and MTOC-associated arrays of contractile fibres where they were first identified (Salisbury et al., 1984). In MTOCs, centrin is a cytologically discrete and functionally important component, required for their duplication, segregation and positioning (Baum et al., 1986; Koblenz et al., 2003; Paoletti et al., 1996; Ruiz et al., 2005; Salisbury et al., 2002; Stemm-Wolf et al., 2005; Wright et al., 1989; Wright et al., 1985). Remarkably, in acentriolar organisms, which form basal bodies only at a specific stage of their life cycle, such as in Naegleria or Marsilea, centrin synthesis strictly correlates with assembly of basal bodies (Klink and Wolniak, 2001; Levy et al., 1996). Centrin is a major constituent of the diverse arrays of MTOC-associated contractile fibres present in unicellular organisms and it mediates Ca^{2+}-induced contractility as shown for the basal-body-associated fibres in *Chlamydomonas* (Hayashi et al., 1998; Salisbury et al., 1987), the spasmonemes in *Vorticella* (Amos et al., 1975; Maciejewski et al., 1999), the myonemes in *Eudiplodinium* (David and Vigues, 1994) and the infraciliary lattice (ICL) in *Paramecium* (Garreau de Loubresse et al., 1991). The discovery in yeast of Sfi1p, a large protein able to bind centrin at many sites (Kilmartin, 2003), has provided a molecular model to account for centrin function in Ca^{2+}-induced contractility and for the dynamic process of spindle pole body, centrosome or basal body duplication (Salisbury, 2004). Evidence supporting this mechanism has recently been obtained in *Paramecium* with the characterisation of a large Sfi1p-like centrin-binding protein required for assembly and function of the contractile ICL (Gogendeau et al., 2007).

Several further discrete localisations have also been identified, in cilia (Gonda et al., 2004; Guerra et al., 2003; LeDizet and Piperno, 1995) and ciliary-derived organelles of sensory cells (Giessl et al., 2006), at the contractile vacuole pores in *Tetrahymena* (Stemm-Wolf et al., 2005) and at the Golgi in *Trypanosoma* (He et al., 2005; Selvapandiyan et al., 2007). Interestingly, if species differ widely in their number of centrin genes (one in yeast, four in mammals, seven in *Leishmania*, at least ten in *Tetrahymena* and 49 in *Paramecium*), when more than a single gene is present, a particular localisation or function may involve either a single or different centrin isotypes and conversely, a particular isotype may show different localisations or functions. In *Trypanosoma*, the same *TbCen1* gene localises at both basal bodies and Golgi and controls their distribution at division (He et al., 2005; Selvapandiyan et al., 2007). In *Paramecium*, two pairs of genes, *PtCen2a/b* and *PtCen3a/b*, code for basal body specific isoforms and their inactivation has no effect on the ICL (Ruiz et al., 2005). Conversely, *ICL1 a/b* code for centrins specific of the ICL and their inactivation has no effect on basal body duplication (Beisson et al., 2001; Ruiz et al., 1998). This diversity of situations

suggests that the ancestral centrin-based contractile system was localised at the central MTOC and controlled its duplication (Ruiz et al., 2005) and cell division. Interesting support for such a view comes from the characterisation in *Chlamydomonas* of a centrin scaffold linking the various 'centrin-containing organelles' (Geimer and Melkonian, 2005). The existence of such centrin-based links between cell organelles and cytoskeletal networks remains to be demonstrated. However, in the case of the *Paramecium* ICL, coordination between the contractile network and the basal bodies is evident because the transcellular organisation of the ICL in polygonal meshes is directly adjusted to the pattern of basal bodies (Beisson et al., 2001).

Within this perspective, and in view of the large number of centrins in *Paramecium* (Ruiz et al., 2005), it seemed of interest to make a complete inventory of the localisation and function of the isotypes present in the ICL. Based on a proteomic analysis of the purified ICL, and on the availability of the complete genome sequence (Arnaiz, 2007; Aury et al., 2006), we have identified 35 isoforms, belonging to 10 centrin subfamilies, here referred to as ICL1a, ICL1e, ICL3a, ICL3b, ICL5, ICL7, ICL8, ICL9, ICL10 and ICL11. In addition to PtCenBP1p, the previously described Sfi1p-like protein shown to form the backbone of the ICL (Gogendeau et al., 2007), we have characterised two members, PtCenBP2p and PtCenBP3p, of a second subfamily of centrin-binding proteins (PtCenBP3). We demonstrated that nine of the ten ICL subfamilies are cytologically and functionally ICL specific. By contrast, the tenth subfamily, ICL1e, which is the most conserved, displays multiple localisations, at the ICL, at basal bodies and at the contractile vacuole pores and plays a role in their biogenesis.

Results

In our previous studies, we showed that the infraciliary lattice (ICL) was composed of a high molecular mass protein and of numerous low molecular mass ones (~20-25 kDa) resolved by two dimensional electrophoresis into six Ca^{2+}-binding spots, labelled by anti-centrin antibodies and four other spots, unable to bind Ca^{2+} and not labelled by anti-centrin antibodies (Garreau de Loubresse et al., 1991). From the N-terminal peptide sequence of the centrin isoform ICL1, we characterised four nearly identical centrin genes: *ICL1a*, *ICL1b*, *ICL1c* and *ICL1d* (Madeddu et al., 1996). The frequent occurrence of such multigene families encoding nearly identical proteins in the *Paramecium* genome, finds its origin in the three successive rounds of whole genome duplication that occurred during *Paramecium tetraurelia* evolution (Aury et al., 2006). Despite gene loss following each round of duplication, over 60% of the genes still have one to several paralogues.

Centrins and centrin-binding proteins are the major constituents of the ICL

In order to further characterise ICL components, we carried out a mass spectrometry analysis of two types of samples: the four non-Ca^{2+}-binding spots observed on 2D gels (Garreau de Loubresse et al., 1988) and whole purified ICL extract. Altogether, 271 unique, high quality peptides (rank 1 with spectra having a score >40) were retained, identified and eventually grouped into 26 protein subfamilies (see supplementary material Fig. S1 and Table S1). We define protein subfamilies as proteins sharing at least one peptide and more than 80% identity at the amino acid level.

These 26 subfamilies included all the previously characterised ICL proteins: PtCenBP1p and the five centrin subfamilies ICL1a, ICL3a, ICL5, ICL7 and ICL8, independently identified from peptide microsequences. In addition, we found two new Sfi1p-like proteins (the subfamily called PtCenBP3 for centrin binding protein 3), five new centrin subfamilies (ICL1e, ICL3b, ICL9, ICL10 and ICL11), and 14 different subfamilies of either known or unknown proteins (supplementary material Table S1). Among the novel protein subfamilies, GSPATP00007371001 and GSPATP00017054001 may be true constituents of the ICL, as they were targeted by a significant number of peptides although they do not appear to be highly expressed proteins as judged by the number of sequenced expressed sequence tags (ESTs) (Aury et al., 2006). By contrast, the α-tubulin, β-tubulin, striatin2 and GSPATP00034697001 subfamilies are probably contaminants because these proteins are highly expressed. Altogether, nearly 75% of the identified peptides belong to the 35 centrin isoforms grouped into 10 subfamilies, and the three Sfi1p-like proteins forming the PtCenBP1 and PtCenBP3 subfamilies.

In this study, we focused on Sfip-1-like proteins and centrins (Table 1). In order to ascertain their role in ICL assembly and function, we localised GFP-tagged proteins (see Materials and Methods) and carried out RNAi experiments, using a representative gene encoding a protein of each subfamily: one gene for the PtCenBP3 subfamily and ten genes for the ten ICL subfamilies.

Three centrin-binding proteins form the backbone of the ICL

PtCenBP1p has previously been characterised as an essential component of the ICL forming the backbone of the network (Gogendeau et al., 2007). The new PtCenBP3 subfamily identified by the proteomic analysis comprises two proteins, PtCenBP2p and PtCenBP3p, which are paralogues of the most recent whole genome duplication sharing 90% amino acid identity and 95% similarity. They could be aligned with PtCenBP1p, on both sides of its large internal motifs (Fig. 1A and supplementary material Fig. S2). These two proteins present a succession of 30 repeats of 23 residues whose consensus is similar to that of the centrin-binding sites found in the yeast or human Sfi1p and in PtCenBP1p (Fig. 1B).

In contrast to the homogenous localisation of PtCenBP1p-GFP along the ICL (Gogendeau et al., 2007), the GFP-PtCenBP3p fusion protein localised preferentially at the mesh junctions in a Y-shaped pattern (Fig. 1C). Moreover, the GFP-PtCenBP3p fusion does not coincide with the network. In cells expressing GFP-PtCenBP3p, double labelling with anti-GFP and anti-centrin antibodies showed that PtCenBP3p localises just beneath the ICL. This localisation was confirmed by confocal microscopy (not shown). This distinctive localisation appears devoid of anti-centrin labelling. These observations reveal an unsuspected complexity of the architecture of the ICL, and show that PtCenBP3p, despite its multiple potential centrin-binding sites, does not bind the centrins recognised by the available antibodies, the monoclonals 20H5 and 1A9, which are specific for a limited set of ICL centrin isoforms (Beisson et al., 2001).

The inactivation of the *PtCenBP2/PtCenBP3* genes was targeted with 587 bp of the *PtCenBP3* sequence. After 24 hours (three cell divisions), the meshes of the ventral side were stripped off and after 48 hours of feeding (5-6 cell fissions, Fig. 1D) most of the network had collapsed into the cytoplasm and remained attached to the cortex only at the poles. This *PtCenBP3*-silenced phenotype indicates that PtCenBP2p and PtCenBP3p are essential for the attachment of the ICL to the cell cortex. As the ICL is the innermost cortical cytoskeletal network and runs at the level of the proximal end of basal bodies and as basal bodies are flanked by an 'ICL

Table 1. Molecular characteristics of the three Sfi1-like proteins and the 35 centrins of the ICL

	Gene name	Protein length (No. amino acids)	Accession no.	Ca^{2+} binding (predicted)
CenBP1	*PtCenBP1*	3894	CR932274	–
CenBP2	*PtCenBP2*	1907	PTETP12700001001	–
	PtCenBP3	1910	PTETP14900001001	–
ICL1a	*Ptcen_icl1a*	181	CAI38926	– + – –
	Ptcen_icl1b	182	CAI38923	– + – –
	Ptcen_icl1c	183	CAI38920	– + – –
	Ptcen_iclid	181	CAI38919	– + – –
	Ptcen_icl1f	183	CAI38922	– + – –
ICL1e	*Ptcen_icl1e*	174	CAI38924	– – – –
	Ptcen_icl1g	174	CAK87884	– – – –
	Ptcen8	178	CAK72443	– – – –
	Ptcen10	174	CAI38927	– – – –
	Ptcen12	174	CAI38936	– – – –
	Ptcen15	178	CAI38934	– – – –
	Ptcen18	174	CAK74252	– – – –
ICL3a	*Ptcen_icl3a*	192	PTETG12700001001	– + + *
	Ptcen_icl3c†	–	CAI44457	–
	Ptcen_icl3d	192	CAI38943	– + + *
	Ptcen_icl3e	190	CAI38941	– + + *
	Ptcen_icl3f	197	CAI38940	– + + *
ICL3b	*Ptcen_icl3b*	194	CAI38944	– * + *
	Ptcen_icl3g	193	CAK62298	– * + *
ICL5	*Ptcen_icl5a*	182	CAI38946	+ – – –
	Ptcen_icl5b	182	CAI38947	+ – – –
	Ptcen_icl6a	184	CAI38945	+ – – –
	Ptcen_icl6b	184	CAI44665	+ – * –
ICL7	*Ptcen_icl7a*	184	CAK88443	– – – –
	Ptcen_icl7b	184	PTETG7800002001	– – – –
ICL8	*Ptcen_icl8a*	184	CAK61997	– – – –
	Ptcen_icl8b	184	CAK65330	– – – –
ICL9	*Ptcen_icl9a*	208	CAI38942	– * * +
	Ptcen_icl9b	208	CAK56833	– * – +
	Ptcen_icl9c	206	CAK77552	– * – +
	Ptcen_icl9d	208	CAK78571	– * – +
ICL10	*Ptcen_icl10a*	206	CAK88399	– + – –
	Ptcen_icl10b	206	CAK58652	– + – –
ICL11	*Ptcen_icl11a*	240	CAK58194	– – – *
	Ptcen_icl11b	240	CAK60788	– – – *
	Ptcen_icl11c‡	240	PTETG11300001001	– – – *

Within each subfamily, the name of each gene, the size in amino acid of the corresponding protein and the accession number are listed. The last column gives a schematic representation of the calcium binding sites of centrins. The EF-hand sequences of each centrin were examined to determine whether they might fix calcium. + represents an expected functional site with a high Ca^{2+} affinity, * a functional site with a low predicted affinity and – sites with no Ca^{2+} affinity. It has been experimentally shown that ICL7p and ICL8p are unable to bind calcium (Garreau de Loubresse et al., 1991). †The *Ptcen_icl3c* is a pseudogene: it presents a mutation, as verified by cDNA sequencing, preventing excision of the first intron and leading to a premature stop codon. ‡The *Ptcen_icl11c* gene presents a noncanonical intron, confirmed by cDNA sequencing, where the canonical GTA 5′-border is replaced by a GCA.

nucleating centre' (Beisson et al., 2001), the *PtCenBP3*-silenced phenotype suggests that PtCenBP3p is an intermediate link between basal bodies and ICL.

The ten centrin subfamilies are phylogenetically diverse

Sequence comparison and phylogenetic analysis (Fig. 2) allowed us to position the ten ICL centrin subfamilies with respect to other known centrins and to the highly conserved Cen2 and Cen3 subfamilies (see supplementary material Figs S3 and S4 and Table S1). Among the subfamilies, some have no orthologues or orthologues only in ciliates (ICL1a, ICL3 ICL5). One subfamily (ICL1e) has orthologues in ciliates and other apicomplexa. Table 1 indicates the characteristics of the 35 centrin isotypes within each of the ten subfamilies. Centrins differ in their ability to bind Ca^{2+}: CrCenp possesses four functional EF-hand domains (Weber et al., 1994) whereas Cdc31p and HsCen2p have only two (Yang et al., 2006). All the ICL centrins have at least one predicted functional Ca^{2+}-binding site (Table 1), except for the different members of the ICL1e, ICL7 and ICL8 subfamilies, which have none.

The ten centrin subfamilies localise at the ICL

In order to ascertain the distribution of individual ICL centrin in the network, a representative of each subfamily was GFP tagged and its localisation examined, except for ICL11. Double staining with antibody against centrin marked the endogenous ICL. Three types of labelling pattern were observed.

In the first type, corresponding to six GFP-fusion constructs with ICL1ap, ICL3bp, ICL5ap, ICL7ap, ICL8ap and ICL9ap respectively, a homogeneous GFP signal along the ICL was observed (Fig. 3A). Owing to the transformation procedure in *Paramecium*, it is possible to obtain a range of clones expressing GFP at different levels. For the six GFP-constructs, strong fluorescence was always correlated with ICL disassembly, whereas clones showing a weaker fluorescence retained a normal ICL. These results suggest that the disassembly of the ICL was due to overexpression of the centrins rather than to the presence of the GFP. Such a dominant negative effect of centrin overexpression has been observed for the basal-body specific centrins 2a and 3b (Ruiz et al., 2005). This effect of overexpression could indicate that ICL

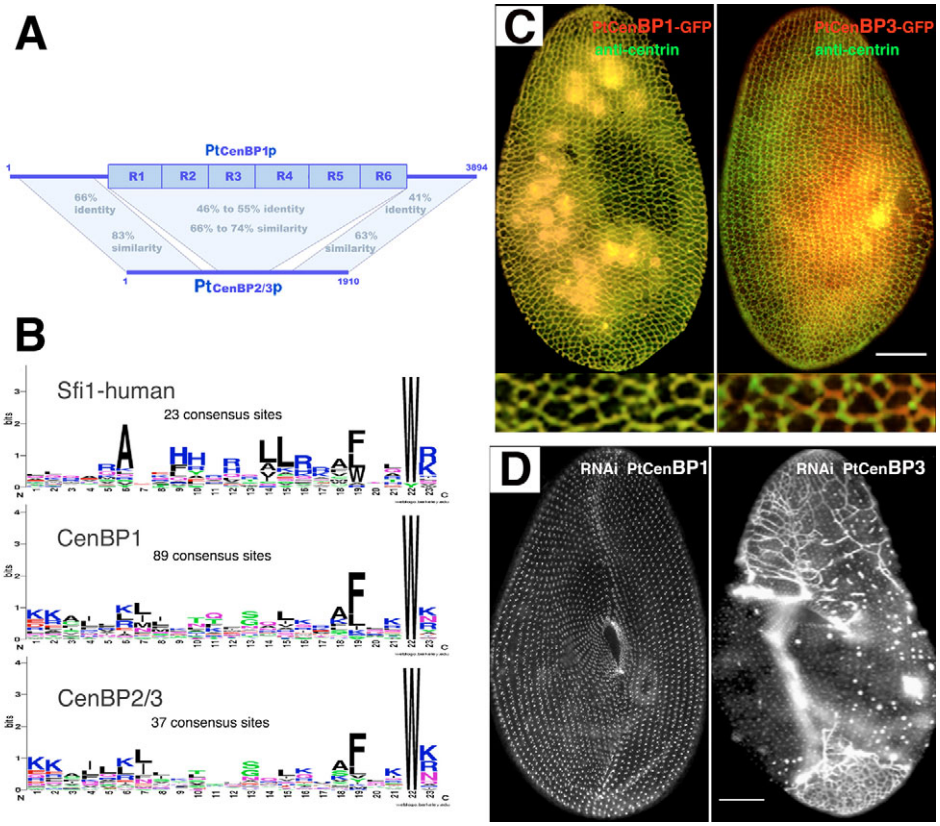

Fig. 1. Comparison of properties of the two families of centrin-binding proteins PtCenBP2/3 and PtCenBP1. (A) Alignment of the primary structures of PtCenBP1p and PtCenBP2/3p shows their regions of homology. R1-R6 correspond to the six identical repeats of 427 amino acids present in PtCenBP1 (Gogendeau et al., 2007). The proteins are highly similar throughout their length, except for the absence of the central repetitions in PtCenBP2/3p. (B) PtCenBP3p displays numerous potential centrin-binding sites that are similar to the centrin-binding consensus defined by Kilmartin (Kilmartin, 2003). The Weblogos of the 30 centrin-binding sites present in PtCenBP3 are compared with those corresponding to the sites present in the human Sfi1p and in PtCenBP1p (Gogendeau et al., 2007). (C) Wild-type cells expressing either GFP-PtCenBP3p (right) or GFP-PtCenBP1p (left) were double-labelled with anti-GFP antibodies (green) and the anti-centrin 1A9 antibody (red). In the GFP-PtCenBP3p expressing cells, the two labels do not colocalise, whereas in the GFP-PtCenBP1p-expressing cells, the two labels colocalise across the network. (D) Wild-type cells were submitted to RNAi targeted either to *PtCENBP3* (right) or *PtCENBP1* (left) and the organisation of the ICL monitored with the anti-centrin antibody 1A9. A collapse of the ICL is observed in a *PtCENBP3*-silenced cell after 48 hours. By contrast, in *PtCENBP1*-silenced cells (after 48 hours of feeding), the ICL is totally disassembled, leaving only small remnants that flank basal bodies. Scale bars: 15 μm.

assembly is regulated by a precise stoichiometry of its components. Localisation of ICL3dp could not be established: in cells expressing the GFP-ICL3d construct, the ICL always disassembled even after transformation with low amounts of DNA (50 ng/μl). Control cells, injected at high concentration of DNA, with the *ICL3d* sequence but without the GFP sequence, did not exhibit any ICL abnormality. These results indicate that the GFP-ICL3d fusion protein has a dominant negative function with respect to ICL assembly or stability, because of the presence of GFP.

A second type of labelling pattern was observed for GFP-ICL10ap. The fluorescence was not homogenous but appeared as beads along the network (Fig. 3B), and the network disassembled after several divisions, suggesting a dominant negative effect of GFP-ICL10ap. When the gene was cloned using the natural *ICL10a* regulatory elements (see Materials and Methods), the observed GFP fluorescence was weaker than previously. ICL integrity was maintained throughout many cell divisions as monitored with an anti-centrin antibody and the beaded pattern was still observed. Our observations indicate that ICL10ap localises at preferential points, ~400 nm apart, along the infraciliary lattice, which might correspond to particular centrin-binding sites on the Sfi1p-like proteins.

A third type of labelling pattern was produced with the GFP-ICL1e construct. As in the case of GFP-ICL10ap, the fluorescence localised as beads along the network. However, the GFP-ICL1ep fluorescence was also detected at the contractile vacuole pores and just anterior of basal bodies (Fig. 3C). The same labelling, with a similar fluorescence intensity, was confirmed when the *GFP-ICL1e* fusion was under the control of its endogenous regulatory sequences (see Materials and Methods). Such a triple localisation was also observed in *Tetrahymena* for the product of the *TtCent4* gene (Stemm-Wolf et al., 2005).

The ten ICL centrin subfamilies are not functionally redundant

In our RNAi experiments, we assumed that all the genes sharing at least one stretch of 23 nucleotides with the target gene are co-silenced. Within each subfamily, silencing of one gene should deplete (at least partially) the products of all members of the subfamily, with the exception of the ICL11 subfamily, because the nucleotide sequences of *ICL11a* and *ICL11c* do not share enough identity. As a control, we used *ND7* silencing which affects trichocyst exocytosis without altering the ICL or any other cellular function (Ruiz et al., 1998). To assess the presence of a functional

ICL, we monitored the network structure by immunolabelling with the anti-centrin 1A9 antibody. Except for *ICL8a,* for which no effect of silencing was observed, all of the RNAi experiments led to a loss of ICL integrity. Interestingly, the patterns of the disorganisation differed according to the targeted gene and four distinct disassembly pathways were observed.

(1) *ICL7a* and *ICL3b* silencing gave the same pattern of ICL disassembly as previously observed in the cases of inactivation of *ICL1a* and *PtCenBP1* (Gogendeau et al., 2007; Ruiz et al., 1998). As shown in Fig. 4A, the transverse part of the meshes was first affected, then disassembly spread throughout the network until only a group of three dots of anti-centrin reactive material remained near each basal body, corresponding to the previously described ICL-organising centres, the ICLOCs (Beisson et al., 2001). Nevertheless, the pace of disorganisation differed according to the gene silenced. While silencing the *ICL7a* subfamily led to complete disassembly after 48 hours of feeding (5-6 cell divisions), ICL3bp depletion never led to complete disassembly and the ICL was able to regenerate after 72 hours. Although we cannot rule out the possibility that *ICL3b* silencing is less efficient, these results suggest that the function of centrins of the ICL3b subfamily can be relayed by other centrins of the ICL, whereas the function of ICL7ap cannot.

(2) *ICL10a* and *ICL11a* silencing gave a second pattern of disassembly (Fig. 4B). After 18 hours of feeding (1-2 fissions), immunolabelling revealed a disrupted ICL with only straight unconnected longitudinal and transversal segments, which suggests a preferential loss of the branching sites where polygonal meshes merge. This phenotype was maintained over 5-6 cell fissions, then the labelling concentrated at the ICLOCs. In the case of *ICL11p*, although one of the three members of the subfamily, the more divergent *ICL11cp*, would not have been expected to be co-silenced, disassembly evolved and went to completion, indicating that ICL11cp is not able to take over the function of ICL11ap/bp.

(3) Under silencing of *ICL3d*, *ICL5a* or *ICL9a* subfamilies, the meshes of the ICL first became thinner, suggesting a decreased number of filaments within the bundles (Fig. 4C). At the same time, large dots appeared at the branching points of the meshes, where large residual aggregates remained after the meshwork was totally disrupted. Eventually, the silenced cells reached the terminal phenotype characterised here by the presence of the ICLOCs near the basal bodies, with some small aggregates remaining visible. In *ICL3d* and *ICL5a* feeding experiments, the disassembly was complete after 48 hours (5-6 cell divisions) and is maintained during several cell divisions. By contrast, *ICL9a* silencing confers a transitory phenotype: the disassembly seems complete after 24 hours of feeding (three divisions) but between 48 and 72 hours (6-10 cell divisions), a nearly normal ICL is recovered.

(4) The phenotype observed after *ICL1e* silencing was remarkable; not only did the pattern of disassembly differ from the previous three (Fig. 5A), but silencing also displayed pleiotropic effects (Fig. 5B-C). The most striking effect was on basal body duplication: their number was reduced, clumps of intracytoplasmic basal bodies appeared and the oral apparatus was disorganised; cells progressively became rounder and smaller, stopped dividing and died. This phenotype was similar to that resulting from the inactivation of the basal-body-specific centrins PtCen2a/b and

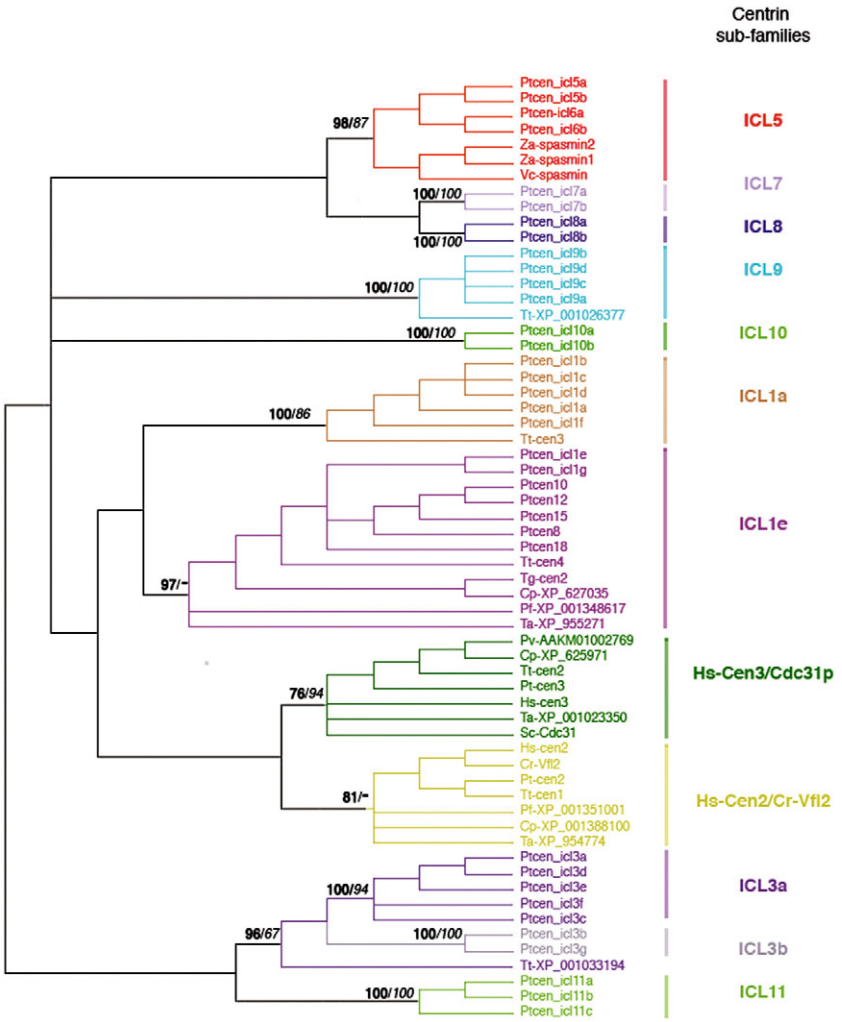

Fig. 2. Phylogenetic tree of ICL centrins. The bootstrap support values from neighbour joining/maximum likelihood analyses are indicated for relevant nodes. /– indicates that some centrins are not grouped by the maximum-likelihood analysis. This tree is supported by the identification of diagnostic amino acid residues specific of each centrin subfamily (supplementary material Fig. S4). Hs-cen2/Cr-VFL2 and Hs-cen3/Cdc31p correspond to the well-defined centriolar centrin subfamilies (Azimzadeh and Bornens, 2004). Cr, *Chlamydomonas reinhardtii*; Cp, *Cryptosporidium parvum*; Hs, *Homo sapiens*; Pf, *Plasmodium falciparum*; Pv, *Plasmodium vivax*; Pt, *Paramecium tetraurelia*; Ta, *Theileria annulata*; Tt, *Tetrahymena thermophila*; Tg, *Toxoplasma gondii*; Vc, *Vorticella convallaria*; Za, *Zoothamnium arbuscula*. The accession numbers of *Paramecium centrins* (named Ptcen_icl or Ptcen) are as in Table 1. Cr-Vfl2=CAA31163; Hs-cen2=AAP35920; Hs-cen3=AAP35334; Pt-cen3=XP_001439003; Pt-cen2=XP_001427485; Tg-cen2=50m03356; Tt-cen1=XP_001019292; Tt-cen2=XP_001470770; Tt-cen3=XP_001026988; Tt-cen4=XP_001023350; Vc-spasmin=AAD00995; Za-spasmin1=BAC43748; Za-spasmin2=BAC43749.

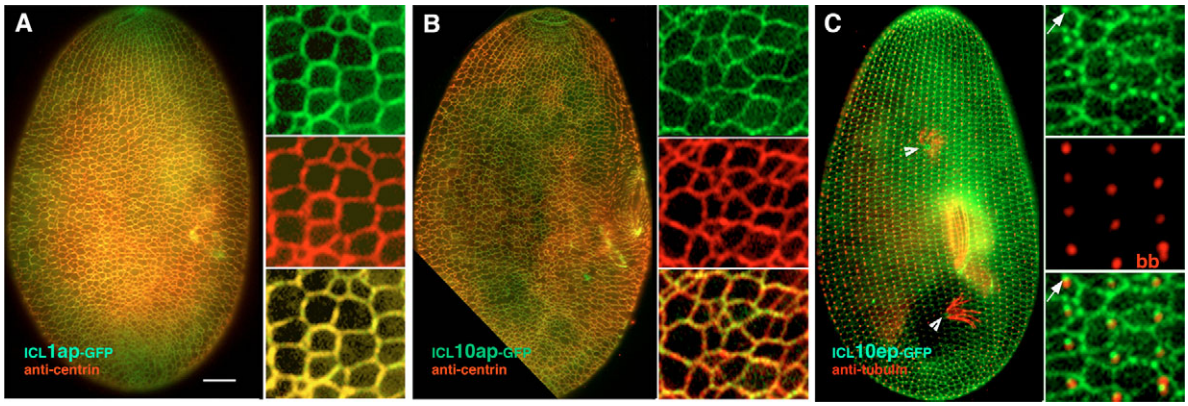

Fig. 3. Localisation of GFP-tagged centrins. For a representative of each centrin subfamily, localisation was monitored in GFP-expressing cells, fixed and double-labelled with an anti-GFP polyclonal antibody (green) and either the monoclonal anti-centrin1A9, specific for the ICL (red) or the monoclonal ID5, which labels essentially the basal bodies (red). To the right of each represented cell, the insets show, from top to bottom, GFP, anti-centrin or anti-tubulin labelling and the merged image of a magnified area. (A) In cells expressing ICL1ap-GFP, the two labels precisely colocalise. (B) In cells expressing ICL10ap-GFP, the GFP labelling clearly shows a beaded pattern, whereas the anti-centrin labelling (specific for the ICL1a subfamily) is continuous along the mesh. (C) In cells expressing ICL1ep-GFP, the GFP signal localises not only at the ICL, with a beaded pattern, but also at the contractile vacuole pores (arrowheads), and anteriorly, in close association with basal bodies (arrows). Scale bar: 15 μm.

PtCen3a/b (Ruiz et al., 2005). In addition, ICL1ep-depleted cells showed a variable number (one to three) of contractile vacuoles (Fig. 5C) instead of two observed in wild-type cells (Fig. 5B). Cells died before the ICL was completely disassembled. These observations showed that, in contrast to all the other centrins present in the ICL, ICL1ep plays multiple functions in the cell, and might act as a physical link between the infraciliary lattice and other cortical organelles, the basal bodies and contractile vacuoles.

Discussion

Based on our previous results (Gogendeau et al., 2007; Klotz et al., 1997) and the combined use of genomics (Arnaiz, 2007; Aury et al., 2006) and proteomics, we have shown that the ICL is composed of three Sfip-like centrin-binding proteins belonging to two subfamilies and 35 centrins belonging to ten subfamilies, three of which have no functional Ca^{2+}-binding site. By GFP-tagging and RNAi experiments, we have demonstrated that these centrins as well as the three Sf1p-like proteins (Gogendeau et al., 2007) localise at the ICL and that there is no functional redundancy among the diverse subfamilies. This multiplicity of isotypes raises questions concerning both their respective function and their evolution. Considering the complex architecture of the ICL, it could be expected that different isotypes might fulfil specialised functions in assembly, stability or contractility of the network as well as in its global architecture. From an evolutionary point of view, it was of interest to examine the relationship between the explosive diversification of centrins and the specialisation of their functions.

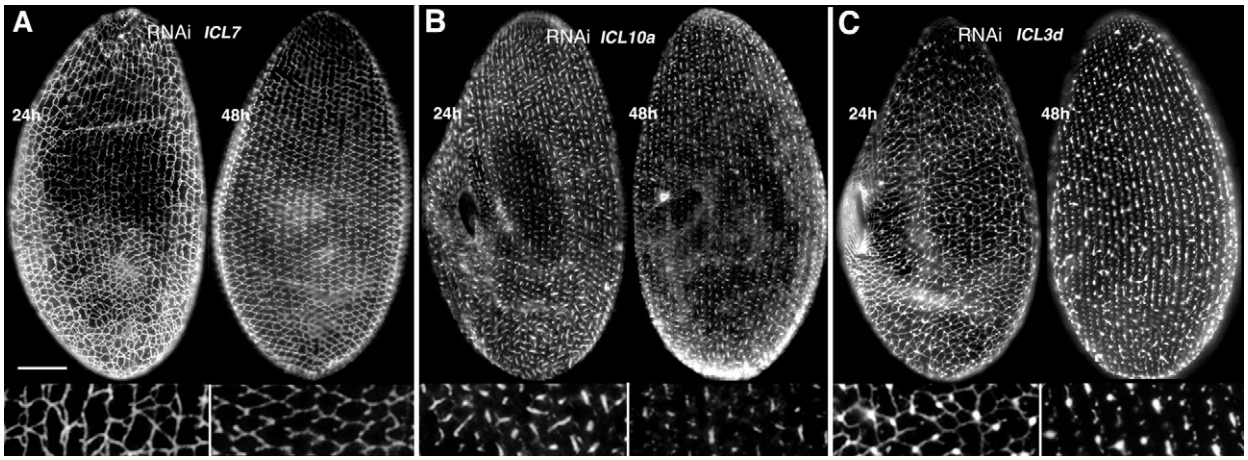

Fig. 4. The effect of centrin depletion is subfamily specific. For all centrins (except ICL8p), RNAi induces a complete disassembly of the ICL observed after a few cell divisions. Although the same terminal phenotype (absence of ICL, small remnants of centrin-containing material near basal bodies) is reached in most cases, the pattern of disassembly, consistently observable throughout the first divisions under RNAi conditions, depends on the targeted subfamily. (A-C) Three of the four recorded modes of disassembly. (A) ICL7p-silenced cells are shown after 24 hours (left) and 48 hours of growth (right): disassembly proceeds progressively and homogeneously. (B) In ICL10ap-silenced cells, thinning of the filament bundles precedes disassembly. (C) In ICL3d-silenced cells, aggregates of ICL material accompany disassembly. The lower panels show enlargements of the above cells. Scale bar: 15 μm.

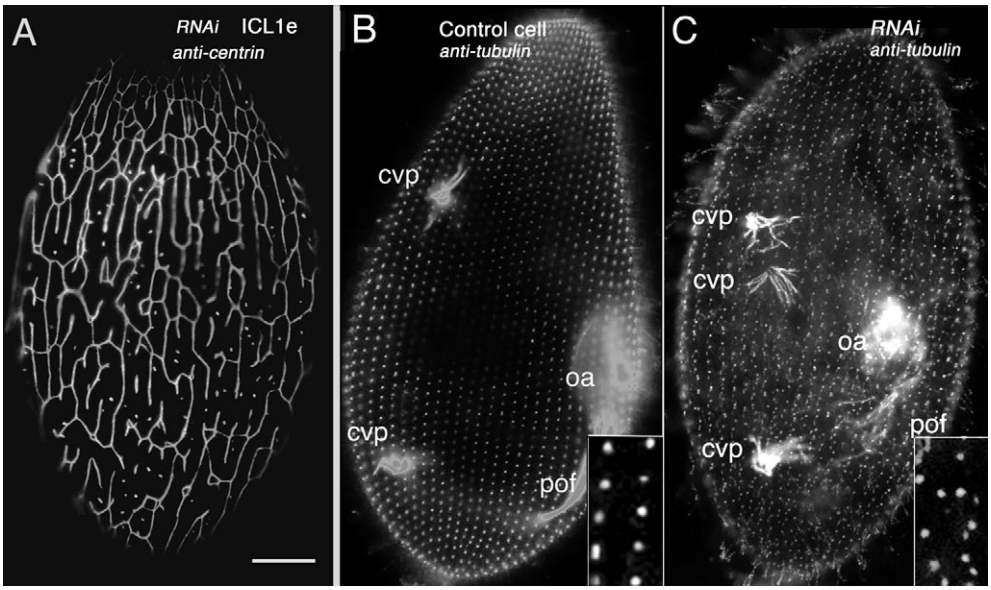

Fig. 5. The pleiotropic effects of ICL1ep depletion. Cells were observed by labelling with either the anti-centrin antibody 1A9 to visualise the ICL (A) or with the anti-tubulin ID5 to visualise microtubular structures and in particular basal bodies (B-C).
(A) Disassembly of the ICL after 24 hours of ICL1ep depletion shows a distinctive pattern compared with those in Fig. 4. No terminal phenotype with complete absence of ICL was observed, because cells die after a few divisions under RNAi conditions.
(C) Disorganisation of the cortex, observed after 48 hours. Comparison with a control cell (B) shows that ICL1ep depletion leads to fewer and misaligned basal bodies, abnormal and reduced oral apparatus (oa) and post-oral microtubules (pof) and an abnormal number of contractile vacuole pores (cvp). Scale bar: 15 μm.

Molecular diversity and ICL biogenesis

Although it was expected that the centrin-binding proteins PtCenBP1p and PtCenBP2p/3p play an essential role in assembly and contractility of the ICL, it is more surprising that all 35 centrins are required for ICL assembly. This is true even for subfamilies of centrins that have no predictable functional Ca^{2+}-binding site (ICL1e, ICL7, ICL8) and are not expected to contribute, at least directly, to the contractility of the network. The demonstration that all components are required for assembly of the network is in agreement with previous data showing that, in the absence of Ca^{2+}, the ICL dissociates into 'elementary complexes' composed of one centrin-binding molecule and representatives of all the centrins (Klotz et al., 1997). Interaction of centrins and centrin-binding proteins thus does not need Ca^{2+}, as also demonstrated for Sfi1p (Kilmartin, 2003; Martinez-Sanz et al., 2006). Thus, there is no reason why ICL1ep, ICL7p or ICL8p would not participate in the elementary complex. The stoichiometry of this elementary complex would then be a key to ICL assembly, in agreement with the dominant negative effect of overexpression observed for ICL1ap, ICL3bp, ICL5ap, ICL7p, ICL8p and ICL9ap. Interestingly, all these isotypes, including the non Ca^{2+}-binding isotypes ICL7p and ICL8p, localise homogeneously along the network and are therefore likely components of the elementary complexes. It can be concluded that the presence of non Ca^{2+}-binding centrin isotypes at some centrin-binding sites of PtCenBP1p or PtCenBP2p/3p does not prevent the contractility of the network. However, there must exist a specificity of binding sites, to ensure precisely the right stoichiometry of both the non-Ca^{2+}-binding and the Ca^{2+}-binding centrin isotypes. In contrast to these isoforms, ICL10p and ICL1ep localise as discrete beads along the network, and their overexpression has little or no effect on the stability of the ICL, two features which suggest that they might contribute to link the elementary complexes rather than be among their constituents.

Further clues as to the function of other ICL constituents come from their particular localisation and/or disassembly pattern. In the case of PtCenBP3p, its localisation beneath the PtCenBP1p backbone and the effect of its depletion indicate a role in anchoring the ICL to the cortex, as well as a tight association with PtCenBP1 complexes. In the case of the centrin isotypes ICL3ap, ICL5p and ICL9ap, their homogeneous localisation along the filaments and the primary effect of their depletion – thinner meshes (Fig. 4B) – suggest a role in lateral interactions between complexes because these interactions are Ca^{2+} dependant and the isotypes possess more than one functional Ca^{2+}-binding site. Finally, ICL1ep is an interesting centrin isotype, the only one that is not ICL specific: in addition to a beaded localisation along the network, like ICL10ap, it is present at contractile vacuole pores and in association with basal bodies. In addition, its depletion affects the duplication/localisation of both organelles. These discrete localisations, two of which are independent of either PtCenBP1p or PtCenBP2p/3p, suggest that ICL1ep is not part of the elementary complexes and may serve as a link between elementary complexes, as proposed for ICL10ap. Its presence at the other two localisations – contractile vacuole pores and basal bodies – suggests a coordinating role between ICL and the other cortical organelles. In conclusion, it would seem that almost all centrin isotypes play a role in the organisation of the network at the molecular and supramolecular level: formation of the elementary complexes, building up and/or branching of filament bundles, and integration within the cortical organisation.

The functional diversity of centrins corresponds to a functional heterogeneity within centrin-binding proteins. Although they are both ICL specific, the PtCenBP1 and PtCenBP3 subfamilies differ, at least in part, in the specificity of their centrin-binding sites: PtCenBP3p does not bind the centrin isoform ICL1ap. It has also been proposed above that a non-random distribution of centrin isotypes along the centrin-binding proteins ensures the required stoichiometry and arrangement of centrins of different Ca^{2+}-binding ability. Although the consensus centrin-binding site is far from strict, and might therefore provide a range of differential affinities to accommodate diverse centrins, differences among centrin-binding sites could hardly have been detected by in vitro studies of the binding of yeast or human centrin to a fragment of Sf1p (Li et al., 2006; Martinez-Sanz et al., 2006). In vitro exploration of the molecular diversity found in *Paramecium* might provide a more sensitive system.

Functional diversity and evolution of centrins and centrin-binding proteins

A number of protozoa show an expanded centrin family: *Plasmodium* possesses eight centrins, *Toxoplasma* 13, *Cryptosporidium* 7 and *Tetrahymena* over 10. In view of the diverse cellular functions of centrins, it can be envisaged that isotype diversification is favoured in unicellular organisms. *Paramecium* possesses 48 centrins, four are basal body specific (Ruiz et al., 2005), two are orthologues of *P. caudatum* centrins involved in a ciliary Ca^{2+} channel (Gonda et al., 2004), 35 are found in the ICL and seven have no known function. However, on the basis of their sequence identity, the 35 ICL centrin genes belong to ten subfamilies. This diversification into ten subfamilies fulfilling nonredundant functions seems to correspond to the morphological complexity of the ICL, a *Paramecium*-specific type of contractile array. In parallel, coevolution of the centrin-binding proteins is likely to have taken place, not only leading to the two subfamilies PtCenBP1 and PtCenBP2/3 with different localisation/function, but also leading to the diversification of the specificities of the centrin-binding sites, which are likely to be involved in the molecular and supramolecular organisation of the ICL.

In contrast to these strictly ICL-specific divergent centrins, the most conserved subfamily, ICL1e, shares the greatest similarity with the centrosomal centrin 2 (Fig. 2). Its orthologue in *Tetrahymena*, TtCen4p, shows three distinct localisations: in the filamentous reticulum at the apical pole, at the contractile vacuole pores and at the base of the kinetodesmal fibres, close to basal bodies (Stemm-Wolf et al., 2005). The *Toxoplasma* orthologue, TgCen2, localises both at the centrioles and in the apical complex, an array of spirally arranged tubulin fibres, which is also the nucleating centre of a microtubule array covering a large part of the cell. *Paramecium* ICL1ep has thus retained the polyvalent localisation present in other species, namely in filamentous/contractile organelles (ICL and the fine filamentous reticulum) and in organelles that are also MTOCs (vacuolar pores, apical complex, basal bodies and centrioles). As centriolar structures and MTOCs in multicellular organisms are generally thought to have evolved from the basal body/axoneme of the unicellular ancestor (Azimzadeh and Bornens, 2004; Azimzadeh and Bornens, 2007), it is reasonable to postulate that, throughout evolution, the most conserved centrin 2 lineage perpetuates conserved functions in basal bodies and in cytoskeleton organisation. Initially concentrated at the single MTOC, these functions might have become spatially and functionally dissociated. In *Trypanosoma*, two isotypes of the cen2 lineage, *TbCen1* and *TbCen2*, localise at both basal bodies and Golgi, and control their distribution at division (He et al., 2005; Selvapandiyan et al., 2007); in *Tetrahymena* and *Paramecium*, TtCen2 and ICL1e, both of the cen2 lineage, presumably fulfil different functions in basal bodies, contractile vacuoles and filamentous arrays. The fact that in addition to nine specialised centrin subfamilies, ICL1ep is maintained as a constitutive element of the ICL in *Paramecium*, strongly suggests that, according to the ancestral dual function in duplication of basal bodies and cytoskeleton, its role may lie in coordinating the organisation of the ICL with the other cortical processes throughout the life cycle.

Materials and Methods

Strains and culture conditions

Stock d4-2 of *Paramecium tetraurelia*, the wild-type reference strain, was used in all feeding experiments. The mutant nd7-1, which carries a recessive monogenic mutation preventing trichocyst discharge (Skouri and Cohen, 1997), a dispensable function under laboratory conditions, was used for the expression of GFP-fusion proteins. Cells were grown at 27°C in a wheat grass infusion (BHB, L'arbre de vie, Luçay Le Male, France or WGP, Pines International, Lawrence, KS) bacterised with *Klebsiella pneumoniae* and supplemented with 0.8 μg/ml β-sitosterol according to standard procedures (Sonneborn, 1970).

Mass spectrometry

Proteins from total ICL extract were digested with trypsin and subsequently reduced and alkylated. The resulting peptide mixture was applied to an RP-18 pre-column (LC Packings) using water containing 0.1% TFA as mobile phase and then transferred to a nano-HPLC RP-18 column (LC Packings, 75 μm inner diameter) using an acetonitrile gradient (0-60% acetonitrile in 35 minutes) in the presence of 0.05% formic acid with a flow rate of 150 nl/minute. Column outlet was directly coupled to the ion source of the LTQ-FTICR (Thermo) ion cyclotron mass spectrometer working in the regime of data dependent MS to MS/MS switch. A blank run ensuring lack of cross contamination from previous samples preceded each analysis. The output lists of precursor and product ions were compared with protein and EST databases using the MASCOT (www.matrixscience.com) search engine (eight-processor version) installed on a local server. For Mascot searches, three databases were used: NCBI nr database, *Paramecium* predicted proteins and *Paramecium* EST (Aury et al., 2006) available from ParameciumDB (Arnaiz, 2007).

Phylogenetic analysis

Neighbour-joining (NJ) reconstructions were performed with the PAUP 4.0 program (Swofford, 1998). Statistical support for the different internal branches was assessed by bootstrap resampling (1000 bootstrap replicates). Maximum likelihood (ML) analyses were performed with PHYML (Guindon and Gascuel, 2003) using the Whelan and Goldman (WAG) amino acid substitution model (Whelan and Goldman, 2001), the frequencies of amino acids being estimated from the data set, and rate heterogeneity across sites being modelled by two rate categories (one constant and eight γ rates). Statistical support for the different internal branches was assessed by bootstrap resampling (150 bootstrap replicates), as implemented in PHYML.

Gene cloning

Restriction sites were introduced at the 5′ and 3′ ends of each gene by PCR amplification, using the oligonucleotides listed in supplementary material Table S2. Amplifications were performed with *Pfx* platinum DNA polymerase (Invitrogen) using standard procedures. Polymerase chain reaction products were subcloned using the pPCRscript™ Cloning Kit (Stratagene) according to the manufacturer's instructions. DNA from positive clones was sequenced and ICL genes were then introduced either into the feeding vector or into the GFP vector using the engineered restriction sites.

RNAi by feeding

Sequences of interest were amplified by PCR and cloned into the feeding vector between two T7 promoters (Timmons and Fire, 1998). For the *PtCenBP3* gene, we amplified a region encompassing positions 5323 to the end of the gene. For centrin genes, the whole sequence from ATG to TGA was amplified. The resulting constructs were used for transformation of HT115, an RNase III-deficient strain of *E. coli* with an isopropyl-β-d-thiogalactopyranoside (IPTG)-inducible T7 polymerase (Sambroock et al., 1989). Wild-type paramecia were incubated into double-stranded RNA-expressing bacteria, as previously described (Galvani and Sperling, 2002) and were transferred daily into fresh feeding medium as needed. Control cells were fed with bacteria carrying the complete coding region of the *ND7* gene, as previously described (Galvani and Sperling, 2002).

GFP constructs

The expression vector for GFP fusion proteins, pPXV-GFP, was previously described (Gogendeau et al., 2005). Each gene was cloned into the *Kpn*I site of pPXV-GFP and placed under the control of the *Paramecium* calmodulin regulatory sequences. GFP was also introduced at the 5′ ends of the ICL1e and ICL10a genes expressed under control of their natural regulatory elements. A *Bgl*II restriction site was engineered 5′ to the start codon by using a two-step PCR. The 5′ regulatory elements (429 bp upstream of the initiator ATG for ICL1e and 133 bp upstream of the initiator for ICL10a) were amplified using primers ICL1e-5′/ICL1e-ATG and ICL10a-5′/ICL10a-ATG (sequences in supplementary material Table S2). Similarly, the coding sequences and the 3′ regulatory elements (353 bp downstream of the TGA for ICL1e and 327 bp downstream of the TGA for ICL10a) were amplified using ICL1e-ATG2/ICL1e-3′ and ICL10a-ATG2/ICL10a-3′. These two purified PCR products were then used as a template for a trans-PCR realised with the primer couples ICL1e-5′/ICL1e-3′ and ICL10a-5′/ICL10a-3′ and cloned into a pPCRscript vector. *Bgl*II restriction sites were added to the GFP sequence, which was then introduced into the engineered *Bgl*II site.

cDNA sequencing

The open reading frames of ICL11c and GSPATG00009965001 genes were amplified by reverse transcriptase polymerase chain reaction (RT-PCR) using total RNA

prepared with the TRIzol (Invitrogen) procedure modified by the addition of glass beads during cell lyses. RT-PCR was performed using a 3′oligo-dTT primer (5′-ggccacgcgtcgactagtacttttttttttttttttt-3′) and the SuperScript™ III reverse transcriptase (Invitrogen). The subsequent PCR (50 μl) was performed with *Pfx* platinum polymerase (Invitrogen) using specific oligonucleotides (supplementary material Table S2). The PCR products were then sequenced to determine the presence or absence of introns.

Transformation

Transformation of *Paramecium* is obtained by micro-injecting the filtered and concentrated plasmid DNA of interest (5 μg/μl) into the macronucleus (Gilley et al., 1988). Microinjection was made under an inverted Nikon phase-contrast microscope, using a Narishige micromanipulation device and an Eppendorf air pressure microinjector. Cell observation was made under a Zeiss Axioskop 2-plus epifluorescence microscope (Zeiss, Oberkochen, Germany) equipped with a Roper Coolsnap-CF intensifying camera using GFP filters. Images were processed using Metamorph software (Universal Imaging, Downington, PA).

Fluorescence microscopy

Immunostaining of cells was carried out as previously described (Klotz et al., 1997). The monoclonal 1A9 raised against *Paramecium* ICL (Beisson et al., 2001) was used at a dilution of 1:200, the monoclonal anti-tubulin antibody 1D5 (Wehland and Weber, 1987) at a dilution 1:1000, the polyclonal anti-GFP antibody from Interchim (Montluçon, France) at 1:500 and secondary antibodies labelled with Alexa Fluor 488 or 546 from Invitrogen-Molecular Probes (Eugene, OR) at a 1:500 dilution. For the GFP recording of living cells, cells were washed twice in Dryl's buffer (Dryl, 1959) containing 0.2% bovine serum albumin (BSA) and then transferred into a small drop on a coverslip and overlaid with paraffin oil. Excess buffer was aspirated until the cells were immobile. Alternatively, GFP-labelled paramecia were fixed in 2.5% formaldehyde before observation or were processed for immunostaining with the polyclonal anti-GFP antibody.

We are much indebted to Constantin Craescu for fruitful discussions and to Anne Fleury for confocal microscopy. We gratefully acknowledge the help of Michel Vervoot for the phylogenetic analysis. We thank Jean Cohen and Linda Sperling for their active and constant interest in this work. We are grateful to Maud Sylvain for DNA sequencing and to Juergen Wehland for supply of the ID5 antibody. This work was supported by the Centre National de la Recherche Scientifique, by grants ACI:IMPBIO 2004 no. 14 and by the ANR contract NT05 _2 –1522. D.G. was supported by the Association de la Recherche Contre le Cancer (A06/3).

References

Amos, W. B., Routledge, L. M. and Yew, F. F. (1975). Calcium-binding proteins in a vorticellid contractile organelle. *J. Cell Sci*. **19**, 203-213.

Arnaiz, O., Cain, S., Cohen, J. and Sperling, L. (2007). ParameciumDB: a community resource that integrates the Paramecium tetraurelia genome sequence with genetic data. *Nucleic Acids Res*. **35**, D439-D444.

Aury, J. M., Jaillon, O., Duret, L., Noel, B., Jubin, C., Porcel, B. M., Segurens, B., Daubin, V., Anthouard, V., Aiach, N. et al. (2006). Global trends of whole-genome duplications revealed by the ciliate *Paramecium tetraurelia*. *Nature* **444**, 171-178.

Azimzadeh, J. and Bornens, M. (2004). The centrosome in evolution. In *Centrosome in Development and Disease* (ed. E. A. Nigg), pp. 93-122. Wiley: Weinheim.

Azimzadeh, J. and Bornens, M. (2007). Structure and duplication of the centrosome. *J. Cell Sci*. **120**, 2139-2142.

Baum, P., Furlong, C. and Byers, B. (1986). Yeast gene required for spindle pole body duplication: homology of its product with Ca2+-binding proteins. *Proc. Natl. Acad. Sci. USA* **83**, 5512-5516.

Beisson, J., Clerot, J. C., Fleury-Aubusson, A., Garreau de Loubresse, N., Ruiz, F. and Klotz, C. (2001). Basal body-associated nucleation center for the centrin-based cortical cytoskeletal network in *Paramecium*. *Protist* **152**, 339-354.

David, C. and Vigues, B. (1994). Calmyonemin: a23 kDa analogue of algal centrin occuring in contractile myonemes of Eudiplodinium magii (ciliate). *Cell Motil. Cytoskeleton* **107**, 9-16.

Dryl, S. (1959). Antigenic transformation in *Paramecium aurelia* after treatment during autogamy and conjugation. *J. Protozool*. **6** Suppl., 25.

Galvani, A. and Sperling, L. (2002). RNA interference by feeding in *Paramecium*. *Trends Genet*. **18**, 11-12.

Garreau de Loubresse, N., Keryer, G., Vigues, B. and and Beisson, J. (1988). A contractile cytoskeletal network of *Paramecium*: the infraciliary lattice. *J. Cell Sci*. **90**, 351-364.

Garreau de Loubresse, N., Klotz, C., Vigues, B., Rutin, B. and Beisson, J. (1991). Ca2+-binding proteins and contractility of the infraciliary lattice in *Paramecium*. *Biol. Cell*. **71**, 217-225.

Geimer, S. and Melkonian, M. (2005). Centrin scaffold in *Chlamydomonas reinhardtii* revealed by immunoelectron microscopy. *Eukaryotic Cell* **4**, 1253-1263.

Giessl, A., Trojan, P., Rausch, S., Pulvermuller, A. and Wolfrum, U. (2006). Centrins, gatekeepers for the light-dependent translocation of transducin through the photoreceptor cell connecting cilium. *Vision Res*. **46**, 4502-4509.

Gilley, D., Preer, J. R., Jr, Aufderheide, K. J. and Polisky, B. (1988). Autonomous replication and addition of telomerelike sequences to DNA microinjected into *Paramecium tetraurelia* macronuclei. *Mol. Cell. Biol*. **8**, 4765-4772.

Gogendeau, D., Keller, A. M., Yanagi, A., Cohen, J. and Koll, F. (2005). Nd6p, a novel protein with RCC1-like domains involved in exocytosis in Paramecium tetraurelia. *Eukaryotic Cell* **4**, 2129-2139.

Gogendeau, D., Beisson, J., Garreau de Loubresse, N., Le Caer, J. P., Ruiz, F., Cohen, J., Sperling, L., Koll, F. and Klotz, C. (2007). A Sfi1p-like Centrin-Binding Protein mediates centrin based Ca2+-dependent contractility in Paramecium. *Eukaryotic Cell* doi:10.1128/EC00197-07.

Gonda, K., Yoshida, A., Oami, K. and Takahashi, M. (2004). Centrin is essential for the activity of the ciliary reversal-coupled voltage-gated Ca2+ channels. *Biochem. Biophys. Res. Commun*. **323**, 891-897.

Guerra, C., Wada, Y., Leick, V., Bell, A. and Satir, P. (2003). Cloning, localization, and axonemal function of Tetrahymena centrin. *Mol. Biol. Cell* **14**, 251-261.

Guindon, S. and Gascuel, O. (2003). A simple, fast, and accurate algorithm to estimate large phylogenies by maximum likelihood. *Syst. Biol*. **52**, 696-704.

Hayashi, M., Yagi, T., Yoshimura, K. and Kamiya, R. (1998). Real-time observation of Ca^{2+}-induced basal body reorientation in Chlamydomonas. *Cell Motil. Cytoskeleton* **41**, 49-56.

He, C. Y., Pypaert, M. and Warren, G. (2005). Golgi duplication in Trypanosoma brucei requires Centrin2. *Science* **310**, 1196-1198.

Kilmartin, J. V. (2003). Sfi1p has conserved centrin-binding sites and an essential function in budding yeast spindle pole body duplication. *J. Cell Biol*. **162**, 1211-1221.

Klink, V. P. and Wolniak, S. M. (2001). Centrin is necessary for the formation of the motile apparatus in spermatids of Marsilea. *Mol. Biol. Cell* **12**, 761-776.

Klotz, C., Garreau de Loubresse, N., Ruiz, F. and Beisson, J. (1997). Genetic evidence for a role of centrin-associated proteins in the organization and dynamics of the infraciliary lattice in Paramecium. *Cell Motil. Cytoskeleton* **38**, 172-186.

Koblenz, B., Schoppmeier, J., Grunow, A. and Lechtreck, K. F. (2003). Centrin deficiency in Chlamydomonas causes defects in basal body replication, segregation and maturation. *J. Cell Sci*. **116**, 2635-2646.

LeDizet, M. and Piperno, G. (1995). The light chain p28 associates with a subset of inner dynein arm heavy chains in Chlamydomonas axonemes. *Mol. Biol. Cell* **6**, 697-711.

Levy, Y. Y., Lai, E. Y., Remillard, S. P., Heintzelman, M. B. and Fulton, C. (1996). Centrin is a conserved protein that forms diverse associations with centrioles and MTOCs in Naegleria and other organisms. *Cell Motil. Cytoskeleton* **33**, 298-323.

Li, S., Sandercock, A. M., Conduit, P., Robinson, C. V., Williams, R. L. and Kilmartin, J. V. (2006). Structural role of Sfi1p-centrin filaments in budding yeast spindle pole body duplication. *J. Cell Biol*. **173**, 867-877.

Maciejewski, J. J., Vacchiano, E. J., McCutcheon, S. M. and Buhse, H. E., Jr (1999). Cloning and expression of a cDNA encoding a Vorticella convallaria spasmin: an EF-hand calcium-binding protein. *J. Eukaryot. Microbiol*. **46**, 165-173.

Madeddu, L., Klotz, C., Le Caer, J. P. and Beisson, J. (1996). Characterization of centrin genes in *Paramecium*. *Eur. J. Biochem*. **238**, 121-128.

Martinez-Sanz, J., Yang, A., Blouquit, Y., Duchambon, P., Assairi, L. and Craescu, C. T. (2006). Binding of human centrin 2 to the centrosomal protein hSfi1. *FEBS J*. **273**, 4504-4515.

Paoletti, A., Moudjou, M., Paintrand, M., Salisbury, J. L. and Bornens, M. (1996). Most of centrin in animal cells is not centrosome-associated and centrosomal centrin is confined to the distal lumen of centrioles. *J. Cell Sci*. **109**, 3089-3102.

Ruiz, F., Vayssie, L., Klotz, C., Sperling, L. and Madeddu, L. (1998). Homology-dependent gene silencing in *Paramecium*. *Mol. Biol. Cell* **9**, 931-943.

Ruiz, F., Garreau de Loubresse, N., Klotz, C., Beisson, J. and Koll, F. (2005). Centrin deficiency in *Paramecium* affects the geometry of basal-body duplication. *Curr. Biol*. **15**, 2097-2106.

Salisbury, J. L. (2004). Centrosomes: Sfi1p and centrin unravel a structural riddle. *Curr. Biol*. **14**, R27-R29.

Salisbury, J. L., Baron, A., Surek, B. and Melkonian, M. (1984). Striated flagellar roots: isolation and partial characterization of a calcium-modulated contractile organelle. *J. Cell Biol*. **99**, 962-970.

Salisbury, J. L., Sanders, M. A. and Harpst, L. (1987). Flagellar root contraction and nuclear movement during flagellar regeneration in *Chlamydomonas reinhardtii*. *J. Cell Biol*. **105**, 1799-1805.

Salisbury, J. L., Suino, K. M., Busby, R. and Springett, M. (2002). Centrin-2 is required for centriole duplication in mammalian cells. *Curr. Biol*. **12**, 1287-1292.

Sambroock, J., Fritsch, E. F. and Maniatis, T. (1989). *Molecular Cloning: A Laboratory Manual*. Cold Spring Harbor, NY: Cold Spring Harbor Laboratory Press.

Selvapandiyan, A., Kumar, P., Morris, J. C., Salisbury, J. L., Wang, C. C. and Nakhasi, H. L. (2007). Centrin1 Is Required for Organelle Segregation and Cytokinesis in Trypanosoma brucei. *Mol. Biol. Cell* **18**, 3290-3301.

Skouri, F. and Cohen, J. (1997). Genetic approach to regulated exocytosis using functional complementation in Paramecium: identification of the ND7 gene required for membrane fusion. *Mol. Biol. Cell* **8**, 1063-1071.

Sonneborn, T. M. (1970). Methods in paramecium research. *Methods Cell Physiol*. **4**, 241-339.

Stemm-Wolf, A. J., Morgan, G., Giddings, T. H., Jr, White, E. A., Marchione, R., McDonald, H. B. and Winey, M. (2005). Basal body duplication and maintenance require one member of the Tetrahymena thermophila centrin gene family. *Mol. Biol. Cell* **16**, 3606-3619.

Swofford, D. L. (1998). *PAUP: Phylogenetic Analysis Using Parsimony (and Other Methods)*. Version 4. Sunderland, MA: Sinauer.

Timmons, L. and Fire. A. (1998). Specific interference by ingested dsRNA. *Nature* **395**, 854.

Weber, C., Lee, V. D., Chazin, W. J. and Huang, B. (1994). High level expression in Escherichia coli and characterization of the EF-hand calcium-binding protein caltractin. *J. Biol. Chem.* **269**, 15795-15802.

Wehland, J. and Weber, K. (1987). Turnover of the carboxy-terminal tyrosine of alpha-tubulin and means of reaching elevated levels of de tyrosination in living cells. *J. Cell Sci.* **88**, 185-203.

Whelan, S. and Goldman, N. (2001). A general empirical model of protein evolution derived from multiple protein families using a maximum-likelihood approach. *Mol. Biol. Evol.* **18**, 691-699.

Wright, R. L., Salisbury, J. and Jarvik, J. W. (1985). A nucleus-basal body connector in Chlamydomonas reinhardtii that may function in basal body localization or segregation. *J. Cell Biol.* **101**, 1903-1912.

Wright, R. L., Adler, S. A., Spanier, J. G. and Jarvik, J. W. (1989). Nucleus-basal body connector in Chlamydomonas: evidence for a role in basal body segregation and against essential roles in mitosis or in determining cell polarity. *Cell Motil. Cytoskeleton* **14**, 516-526.

Yang, A., Miron, S., Mouawad, L., Duchambon, P., Blouquit, Y. and Craescu, C. T. (2006). Flexibility and plasticity of human centrin 2 binding to the xeroderma pigmentosum group C protein (XPC) from nuclear excision repair. *Biochemistry* **45**, 3653-3663.